Journal of Integrative Agriculture 2026, 25(3): 965–976

Available online at ScienceDirect

Journal of Integrative Agriculture



RESEARCH ARTICLE

Critical role of outside xylem hydraulic conductance in regulating stomatal conductance and water use efficiency in cotton across different planting densities

Yunrui Chen[1*], Dayong Fan[2*], Ziliang Li[1], Yujie Zhang[1], Yang He[1], Minzhi Chen[1], Wangfeng Zhang[1], Yali Zhang[1#]

[1] *Key Laboratory of Oasis Eco-agriculture, Xinjiang Production and Construction Corps, Shihezi University, Shihezi 832003, China*
[2] *State Key Laboratory of Efficient Production of Forest Resources, Beijing Forestry University, Beijing 100083, China*

Highlights

- New perspective on the relationship between leaf hydraulic conductance (K_{leaf}) and stomatal conductance (g_s): This study provides a novel perspective by partitioning K_{leaf} into inside-xylem (K_x) and outside-xylem (K_{ox}), elucidating the regulatory mechanisms of K_{leaf} on g_s.
- Optimizing planting density to enhance water use efficiency: The research demonstrates that K_{ox} is significantly positively correlated with g_s, enabling cotton to maintain leaf photosynthetic rate (A_N) while reducing transpirational water loss, thus improving water use efficiency (WUE) across a gradient of planting densities.
- Structural basis and influencing factors of K_{ox}: K_{ox} is significantly influenced by leaf anatomical traits, particularly leaf thickness and the volume fraction of inter-cellular air space; it exhibits a significant negative correlation with WUE as planting density increases, underscoring the importance of leaf hydraulic properties for effective plant water management.

Abstract

Hydraulic theory predicts a positive coupling between leaf hydraulic conductance (K_{leaf}) and stomatal conductance (g_s); however, this theory has not been fully supported by observations, and underlying mechanisms are poorly understood. Partitioning K_{leaf} into inside-xylem (K_x) and outside-xylem (K_{ox}) components offers a refined framework for elucidating the regulation of g_s by leaf hydraulics. While optimal planting density may enhance water use efficiency (WUE) through modulation of g_s, corresponding changes in leaf hydraulic properties and their influence on gas exchange remain unclear. We examined relationships among K_x, K_{ox}, g_s, leaf photosynthetic rate (A_N), and WUE, and analyzed the structural determinants of K_{ox} in cotton grown under eight planting densities: 12, 18, 24, 36, 48, 60, 72, and 84 plants m^{-2}. Results showed that as planting density increased, K_{leaf} and A_N remained stable, whereas K_{ox} and g_s declined significantly. Leaf thickness and the volume fraction of inter-cellular air space were key structural factors influencing K_{ox}. Neither K_{leaf} nor K_x correlated with A_N or g_s; however, K_{ox} exhibited a significant positive correlation with g_s. Furthermore, K_{ox} was negatively correlated with WUE. These findings indicate that K_{ox} modulates g_s to minimize water loss without compromising A_N, thereby enhancing WUE in cotton across varying planting densities.

Keywords: cotton, leaf hydraulic conductance, water use efficiency, planting density, mesophyll structure, stomatal conductance

1. Introduction

Leaf stomatal opening enables CO_2 diffusion into the leaf, while simultaneously causing inevitable water loss *via* transpiration. Transpiration necessitates a continuous supply of water through the leaf hydraulic system to compensate for these losses. Consequently, leaf hydraulic conductance

Received 28 May 2024; Received in revised form 5 September 2024; Accepted 24 September 2024; Available online 5 November 2024
[#]Correspondence Yali Zhang, E-mail: zhangyali_cn@foxmail.com, zhangyali_shzu@163.com
[*] These authors contributed equally to this study.

© 2026 CAAS. Publishing services by Elsevier B.V. on behalf of KeAi Communications Co. Ltd. This is an open access article under the CC BY-NC-ND license (http://creativecommons.org/licenses/by-nc-nd/4.0/). Peer review under responsibility of Editorial Board of *Journal of Integrative Agriculture*.
doi: 10.1016/j.jia.2024.11.012

(K_{leaf}), defined as the rate of liquid water movement through the leaf, should coordinate with stomatal conductance (g_s), which represents the rate of gaseous water vapor diffusion. Thus, the coordination between K_{leaf} and g_s can influence leaf photosynthetic rate (A_N) (Sack and Holbrook 2006; Scoffoni *et al.* 2016). However, current findings regarding the relationship between K_{leaf} and g_s remain inconsistent and poorly understood. Some studies report a strong coupling between K_{leaf} and g_s (Theroux-Rancourt *et al.* 2013; Huang *et al.* 2017; Xiong *et al.* 2017, 2018), whereas others find no significant association (Locke and Ort 2014; Maria 2016; Ocheltree *et al.* 2016; Corso *et al.* 2020). As a result, the functional linkage between K_{leaf} and g_s remains debated.

This uncertainty likely arises because most prior studies did not differentiate the components of K_{leaf}. Based on the analogy between water flow through a leaf and electric current governed by Ohm's law in an electrical circuit (Sack and Holbrook 2006), K_{leaf} can be partitioned into two components: leaf hydraulic conductance inside-xylem (K_x) and leaf hydraulic conductance outside-xylem (K_{ox}) (Sack and Holbrook 2006). Previous research indicates that the relationships among K_x, K_{ox}, and g_s are complex. For instance, studies on different rice genotypes have revealed a significant correlation between K_{leaf} and g_s (Xiong *et al.* 2015), yet neither K_x nor K_{ox} correlated with g_s (Xiong *et al.* 2017). Liu *et al.* (2019) examined multiple tree species and found that both K_x and K_{ox} were positively correlated with g_s. Conversely, work across diverse plant species suggests that K_{leaf} affects g_s primarily through K_{ox}, rather than K_x (Lu *et al.* 2019). These discrepancies may stem from genotypic variation and/or environmental interactions among species. Therefore, accounting for genotype-specific effects is essential when interpreting outcomes.

As evident from existing literature, results concerning the influence of K_{leaf} components on g_s vary widely. Notably, some studies indicate that inside-xylem hydraulic resistance (R_x=1/K_x) accounts for approximately 27% of total leaf hydraulic resistance (Boyer 1974; Salleo *et al.* 2003; Trifilo *et al.* 2003; Cochard *et al.* 2004), with relatively minor interspecific variation. In contrast, outside-xylem hydraulic resistance (R_{ox}=1/K_{ox}) exhibits greater leaf hydraulic variability across species (R_{leaf}), contributing 8–81% of total resistance (Sack and Holbrook 2006; Scoffoni and Sack 2015; Xiong *et al.* 2015). This variability supports the intuitive hypothesis that K_{ox} may be more closely linked to g_s than K_x. Theoretical models suggest that effective water transport encounters a series of serial resistances along the pathway from leaf veins to substomatal cavities prior to transpiration. The analogy between water flow in leaves and electrical current described by Ohm's law in an electrical circuit is notable (Sack and Holbrook 2006). In vascular plant leaves, at least three key factors transport pathway. First, vein diameter influences conductivity, with K_{leaf} scaling positively with the fourth power of vessel diameter (Sterck *et al.* 2008; Pittermann *et al.* 2011); however, xylem water transport efficiency often appears redundant and dynamically regulated (Sack and Holbrook 2006; Sack *et al.* 2008). Second, the water transport route from the vascular bundle sheath to the nearest substomatal cavity constitutes a critical segment (Scoffoni 2015). This 'last mile' involves a complex anatomical path and represents a major contributor to overall leaf hydraulic resistance. Third, resistance to water vapor diffusion occurs at the stomata themselves, where the reciprocal of stomatal resistance corresponds directly to g_s, representing the final 'current' in the hydraulic circuit. Given this framework, larger resistance components are expected to exert proportionally greater control over the final flux (g_s). Hence, mesophyll water transport efficiency (1/R_{ox}) is likely more tightly correlated with g_s. These observations and theoretical considerations suggest that K_{ox} may exhibit a stronger relationship with g_s than K_x; however, further experimental validation is required to confirm this hypothesis.

The variability in R_x and R_{ox} is associated with leaf anatomical structure. Leaf vein density, defined as the length of leaf veins per unit leaf area (VLA, mm cm^{-2}), is considered a key anatomical trait influencing K_{leaf} (Ueno *et al.* 2006; Blonder *et al.* 2011). Early studies indicated that higher K_{leaf} is typically associated with greater VLA (Aasamaa *et al.* 2001; Sack *et al.* 2004). Increased VLA provides additional parallel pathways for water movement, thereby enhancing K_x. Additionally, previous research has clarified how xylem conduit number and diameter affect K_x (North *et al.* 2013). Meanwhile, K_{ox} encompasses both non-vascular intracellular water transport and intracellular water transport within mesophyll tissue (Buckley *et al.* 2015). Research on the impact of mesophyll structure on K_{ox} has a long history, as internal anatomy critically determines sites of evaporation and locations of major hydraulic resistance (Meidner 1976; Tyree and Yianoulis 1980). Current evidence indicates that major structural determinants of K_{ox} include vascular sheath cell size, leaf thickness, mesophyll tissue thickness, mesophyll cell dimensions, and mesophyll porosity (Sack and Frole 2006; Buckley *et al.* 2015). Although extensive research has addressed the structural regulation of K_{ox}, most studies have focused on interspecific comparisons. In contrast, investigations into leaf structural variation within a single species — particularly cultivated crops under differing environmental conditions — and its effect on K_{ox} remain limited.

Optimal planting density can effectively enhance g_s and photosynthetic rate in crops, enabling synergistic improvements in yield and water use efficiency (WUE) (Ruiz and Bertero 2008; Toillon *et al.* 2013; Yao *et al.* 2016; Zhang *et al.* 2016; Sun *et al.* 2019). Current research has explored mechanisms by which planting density regulates photosynthesis and WUE, focusing mainly on stomatal traits affecting g_s, such as stomatal density and size (Corrêa *et al.* 2015; Yang *et al.* 2022), and their impacts on photosynthetic rate (Gonzalez *et al.* 2022; Yang *et al.* 2022). However, considering only stomatal morphology is insufficient for fully explaining regulation of photosynthesis and WUE; it is equally important to consider the support provided by leaf water transport capacity during stomatal opening (Xiong *et al.* 2017). Studies on cultivated crops show that K_{leaf} influences g_s in different rice genotypes (Xiong *et al.* 2015) whereas K_x and K_{ox} do not correlate with g_s (Xiong *et al.* 2017). In contrast, research on monocots and dicots demonstrates that both K_x and K_{ox} regulate g_s under varying soil potassium levels, revealing the hydraulic-anatomical basis of stomatal regulation (Lu *et al.* 2019). Nevertheless, no study has

reported the relationship between leaf hydraulic traits and g_s under varying planting densities. While some work has examined leaf vascular structure under different planting conditions (Corrêa *et al.* 2015), the underlying regulatory mechanisms of g_s remain unclear.

In this study, we use cotton — a globally significant natural fiber and economic crop — as our experimental system. We investigate the hydraulic mechanisms underlying improved WUE in cotton by altering the planting density of a single cultivar, thereby inducing changes in leaf hydraulic properties and gas exchange characteristics. We hypothesize that: (1) Due to the complexity of extraveinal water transport pathways in mesophyll tissue, R_{ox} constitutes a dominant component of total resistance in *Gossypium hirsutum* L., resulting in a closer relationship between K_{ox} and g_s compared to K_{leaf} or K_x; and (2) leaf thickness determines the linear distance of extraveinal water transport, and changes in leaf thickness are commonly accompanied by shifts in mesophyll porosity, suggesting that both leaf thickness and mesophyll porosity are key factors regulating K_{ox}.

2. Materials and methods

2.1. Experimental design

Field experiments were conducted in 2020 at the Ulanwusu Ecological and Agricultural Meteorological Experimental Station in Xinjiang, China (44°17′N, 85°49′E). The soil texture of the experimental field was clay. A completely randomized block design was employed using upland cotton (*G. hirsutum* L. cv. Xinluzao 72) as the experimental material, with a total of eight planting density treatments. The planting density gradient, from low to high, was as follows: (1) 12 plants m^{-2}; (2) 18 plants m^{-2}; (3) 24 plants m^{-2}; (4) 36 plants m^{-2}; (5) 48 plants m^{-2}; (6) 60 plants m^{-2}; (7) 72 plants m^{-2}; (8) 84 plants m^{-2}. Prior to sowing, nitrogen (150 kg ha^{-1} as urea) and phosphorus (225 kg ha^{-1} as KH_2PO_4) were applied. The fertilizers and crop residues were incorporated into the soil, and the experimental plots were then covered with plastic film. Sowing was carried out on April 24, 2020, by manually punching holes in the film and planting cotton seeds. Irrigation was performed using subsurface drip irrigation beneath the plastic film, configured in a 'one film, three drip lines, six rows of cotton' layout — indicating three drip lines under each film and six rows of cotton per film, corresponding to a (66+10) cm row spacing. All treatments received the same amount of water two days after sowing to promote uniform germination. During the growing season, irrigation was applied as needed 9 times, with a total water application of 2,733 m^3 ha^{-1}. The first irrigation occurred on June 9, 2020, followed by subsequent applications on June 21, June 30, July 9, July 18, July 27, August 6, August 15, and August 25. Nitrogen fertilizer (urea at 520 kg N ha^{-1}) and phosphorus fertilizer (KH_2PO_4 at 158 kg P ha^{-1}) were uniformly applied across all treatments. Uniform irrigation, fertilization, and chemical control practices were maintained throughout the growth period.

2.2. Data collection

Data collection for all experimental parameters began on July 10, 2020, during the flowering stage of cotton. The measured parameters are described below:

Measurement of leaf hydraulic conductance Mature leaves were selected to measure K_{leaf} using the evaporative flux method (EFM), where K_{leaf} is calculated as the ratio of transpiration rate (E, mmol m^{-2} s^{-1}) to the leaf water potential gradient ($\Delta\psi_{leaf}$, MPa) (Sack and Scoffoni 2012). Briefly, cotton shoots bearing at least three mature leaves were cut and immediately placed in water, then recut underwater to eliminate embolism formation. The shoots were enclosed in black plastic bag and equilibrated in the laboratory for over 5 hours (overnight in this study). Leaf petioles were cut underwater and connected to pre-filled plastic tubing submerged in a water bath. The excised leaves were exposed to artificial light with an intensity of approximately 2,000 μmol m^{-2} s^{-1} at the leaf surface. Environmental temperature was maintained at 28–30°C. A balance (Sartorius, BSA224S, Germany) recorded weight changes over time, and the slope of the stable phase indicated the flow rate (E). Each leaf was monitored for 15 min after stabilization. Subsequently, leaf area, length, and width were measured, and leaf water potential (ψ_{leaf}) was determined using a pressure chamber (SKPM1400–50, Skye Instruments, Llandrindod Wells, UK). Given the negligible resistance of the water tubing, it was excluded from the calculation of K_{leaf}, which follows the eq.:

$$K_{leaf}=\frac{E}{\Psi_{water}-\Psi_{leaf}} \quad (1)$$

where E represents the steady-state leaf transpiration rate measured gravimetrically; Ψ_{water} denotes the water potential of distilled water, assumed to be 0 MPa in previous studies.

Simulation of leaf hydraulic conductance inside xylem In this study, K_x (mmol m^{-2} s^{-1} MPa^{-1}) in leaf veins was estimated using the Hagen-Poiseuille eq. (North *et al.* 2013):

$$K_x=\frac{\pi(a^2\cdot b^2)}{128\,\eta}\cdot n\cdot VLA_{minor} \quad (2)$$

In this context, a represents the height of conduits in small leaf veins (3rd order and higher), measured in micrometers (μm), while b corresponds to their width, also in micrometers (μm). n indicates the number of conduits within a vascular bundle, and η denotes the dynamic viscosity of water, taken as 8.324×10^{-3} Pa s at 28°C. Hydraulic conductivity was first calculated for individual vascular bundles, and mean values of K_x were subsequently determined. Previous studies have demonstrated that primary leaf veins primarily contribute to mechanical support, whereas the main resistance to water flow occurs in the small leaf veins (Sack *et al.* 2002, 2004). Therefore, this study employs conduits in leaf veins of the 3rd order and above to calculate leaf vein hydraulic conductance.

Simulation of leaf hydraulic conductance outside xylem The leaf hydraulic conductance outside xylem is denoted as K_{ox} (mmol m^{-2} s^{-1} MPa^{-1}). K_{ox} was derived from measured K_{leaf} and K_x the series resistance model:

$$\frac{1}{K_{leaf}}=\frac{1}{K_x}+\frac{1}{K_{ox}} \quad (3)$$

Hence, the expression for calculating K_{ox} is:

$$K_{ox}=\frac{K_{leaf}\cdot K_x}{K_x-K_{leaf}} \quad (4)$$

Measurement of leaf thickness and leaf structure For each

treatment, 3–5 leaves samples were collected. Tissue sections measuring 10 mm in length and 4 mm in width were excised from positions located one-third of the distance from the leaf tip. These samples were fixed in formalin-acetic acid-alcohol fixative (FAA) solution, dehydrated through an ethanol series, cleared, and embedded in paraffin. Cross-sections were double-stained with safranin and alcian blue and mounted with neutral resin. The sealed sections were dried in an oven at 37°C. Prepared slides were observed and photographed under an optical microscope (Olympus, BX51, Japan). Using ImageJ software (National Institute of Health, Bethesda, MD, USA), the distance between the upper and lower epidermis was measured at a minimum of five equidistant points per cross-section and averaged as leaf thickness (LT, mm). Additionally, the thicknesses of the palisade (PT, mm) and spongy tissue thickness (ST, mm) were quantified separately. Clear areas of a certain size were selected from cross-sections of both palisade and spongy tissues in each slice. The areas of all cells within the selected regions were quantified, and the average values were recorded as palisade tissue cell area (PTCA) and spongy tissue cell area (STCA). At least five fields of view were quantified for each slice. Using ImageJ software (National Institute of Health, Bethesda, MD, USA), the total cross-sectional area of the leaf mesophyll tissue (S_{mes}) and the intercellular air space area (S_{IAS}) were measured (Lu *et al.* 2019). The volume fraction of intercellular air space (f_{IAS}) was calculated as:

$$f_{IAS}=\frac{S_{IAS}}{S_{mes}} \quad (5)$$

Similarly, the calculations for f_{IAS_PT} are done using the respective cross-sectional areas of the leaf palisade tissue and the intercellular air space area; the calculations for f_{IAS_ST} are done using the cross-sectional area of the leaf spongy tissue and the intercellular air space area, respectively.

Measurement of xylem structure For each treatment, 3–5 leaves were sampled, and cross-sections of the leaves were prepared, avoiding the first- and second-order veins. Sections were fixed in FAA solution, dehydrated, cleared, and embedded in paraffin. Double staining with safranin and alcian blue was performed, and sections were sealed with neutral resin. Slides were examined and imaged under an optical microscope (Olympus, BX51, Japan). Using ImageJ software (National Institute of Health, Bethesda, MD, USA), conduit height (*a*, μm), width (*b*, μm), and number (*n*) were measured in all visible vascular bundles per cross-section.

Measurement of VAL For each treatment, 3–5 mature leaves were selected. At a position one-third from the leaf tip, leaf tissues with dimensions of 7 mm×7 mm in width were cut and placed in a water bath at 65°C for 12 h. Afterward, the samples were rinsed with 80% ethanol, heated in a 65°C water bath for 1–2 h, and then rinsed with 10% NaOH. After thorough cleaning, the samples were stained with safranin, dehydrated in a gradient of alcohol, and sectioned for observation and photography. At least three clear fields of view were selected for each section, and ImageJ (National Institute of Health, Bethesda, MD, USA) was used to quantify the length of leaf veins in each field of view, thus calculating VLA (mm mm^{-2}).

Leaf gas exchange parameters and leaf intrinsic WUE measurement Gas exchange in leaves was measured from 11:00 to 14:00 h using an LI-6400 portable infrared gas exchange analysis system (LI-COR Inc., Lincoln, USA) under conditions of light saturation (PPFD of 2,000 μmol m^{-2} s^{-1}). For carbon dioxide concentration, the reference chamber's CO_2 level (C_a) was maintained at 400 μmol CO_2 mol^{-1}. The leaf chamber's temperature and relative humidity were strictly controlled at 30°C and 45%, respectively. Measurements were taken on fully expanded young leaves, randomly selected for each treatment. Four separate measurements were made for each treatment, each on a different plant. To ensure consistent lighting conditions, photosynthetic parameters were assessed on the same leaf area without altering its position.

Leaf intrinsic water use efficiency (WUE_i) was calculated using measurements obtained from the LI-6400 gas exchange analysis system (LI-COR Inc., Lincoln, USA). Leaf photosynthetic rate (A_N) and stomatal conductance (g_s) were used in the following formula:

$$WUE_i=\frac{A_N}{g_s} \quad (6)$$

Long-term WUE of leaves The leaf samples, after removing the petioles , were dried at 60°C, and then ground into fine powder after removing the midrib. All samples were measured at the Xinjiang Institute of Ecology and Geography and combusted in an elemental analyzer (EA 1112 Series, Thermo Flash, Bremen, Germany). The stable carbon isotope ratio (^{13}C to ^{12}C) of leaf tissues relative to the Pee Dee Belemnite standard (VPDB) was determined using a stable isotope ratio mass spectrometer (Delta Plus, Thermo Fisher Scientific, Bremen, Germany). The results were reported as $\delta^{13}C$, in per mil (‰), which indicates the comprehensive leaf WUE (Farquhar and Richards 1984).

Determination of stomatal structure The nail polish imprint method involved applying colorless and transparent nail polish to the 1/3 portion of mature leaves near the midrib. After allowing it to dry completely, temporary mounts were created and photographed under an optical microscope (Olympus BX51). For each treatment, at least six stomatal mounts were prepared from different leaves. ImageJ software was utilized to quantify stomatal area, and the mean value was recorded as stomatal size (SS). Different known area regions were selected to count the number of stomata, resulting in stomatal density (SD). Stomatal length (L_s) was quantified, and stomatal pore area index (SPI) was calculated as follows (Sack *et al.* 2003):

$$SPI=L_S^2 \cdot SD \cdot 10^{-4} \quad (7)$$

2.3. Statistical analysis

SPSS 21.0 (SPSS, Chicago, USA) was used to conduct One-way ANOVA to test the differences in measured traits among different treatment. Regression analyses were performed with mean values to test the correlations between parameters. All regressions were fitted by linear model. Regression lines was shown for $P<0.05$.

3. Results

3.1. Variation in leaf water transport efficiency and resistance under different planting densities

In this study, substantial variations in leaf hydraulic traits were observed under different planting densities for the same cotton species (Table 1). As shown in Table 1, K_{leaf} did not exhibit significant differences between treatments, but K_x and K_{ox} showed significant variations among treatments. K_x displayed a significant range of variation, ranging from 26.12 μmol m^{-2} s^{-1} MPa^{-1} at 48 plants m^{-2} to 44.97 μmol m^{-2} s^{-1} MPa^{-1} at 72 plants m^{-2}, representing a 1.72-fold change. The variation in K_{ox} was smaller, ranging from 8.94 μmol m^{-2} s^{-1} MPa^{-1} at 72 plants m^{-2} to 12.44 μmol m^{-2} s^{-1} MPa^{-1} at the lowest planting density (12 plants m^{-2}), with a 1.39-fold change. The selected cotton genotypes showed significant differences in the percentage of leaf hydraulic resistance in both the inside ($R_x/R_{leaf}=K_{leaf}/K_x$) and outside ($R_{ox}/R_{leaf}=K_{leaf}/K_{ox}$) xylem under different planting densities. The percentage of inside xylem hydraulic resistance ranged from a minimum of 17.37% at 72 plants m^{-2} to 29.58% at 12 plants m^{-2}, representingindicating a 1.7-fold change. The variation in outside xylem hydraulic resistance was only 1.17-fold, ranging from a minimum of 70.42% at 12 plants m^{-2} to 82.63% at 72 plants m^{-2}. In terms of the percentage of leaf water resistance attributed to the inside and outside xylem, R_{ox}/R_{leaf} was significantly lower in the 12 plants m^{-2} compared to other treatments, showing an overall increasing trend. Conversely, R_x/R_{leaf} was significantly higher in the lowest-density treatment compared to other treatments, demonstrating an overall decreasing trend (Table 1; Fig. 1). Overall, R_{ox} constituted the primary source of leaf water transport resistance.

3.2. Effects of leaf hydraulic properties on g_s

Planting density significantly influenced g_s, with the highest g_s observed at 12 plants m^{-2}, where the highest g_s was 1.45 times that of the lowest g_s (Appendix A). Further investigation from the perspective of leaf water balance revealed a significant positive correlation between K_{ox} and g_s (Fig. 2-C), while there was no apparent correlation between K_{leaf} and K_x with g_s (Fig. 2-A and B). This suggests that the efficiency of water transport outside leaf veins is the primary factor limiting leaf water diffusion.

Table 1 Effects of planting density (PD) on hydraulic functional traits of cotton leaves[1)]

PD (plants m^{-2})	K_{leaf} (μmol m^{-2} s^{-1} MPa^{-1})	K_x (μmol m^{-2} s^{-1} MPa^{-1})	K_{ox} (μmol m^{-2} s^{-1} MPa^{-1})	R_x/R_{leaf} (%)	R_{ox}/R_{leaf} (%)
12	8.03±0.10 a	27.70±3.97 c	11.43±0.61 ab	29.58±4.32 a	70.42±4.32 b
18	9.53±0.19 a	40.88±1.10 ab	12.44±0.39 a	23.33±0.98 ab	76.66±0.98 ab
24	7.97±0.18 a	30.98±2.49 c	10.78±0.54 ab	24.52±1.71 ab	75.48±1.71 ab
36	7.56±0.04 a	32.24±0.31 bc	9.91±0.01 ab	23.51±0.15 ab	76.49±0.15 ab
48	7.33±1.09 a	26.12±5.13 c	10.24±1.45 ab	29.07±6.77 a	71.60±2.77 b
60	7.78±0.40 a	43.52±6.00 a	9.58±0.94 b	18.40±3.71 b	81.60±3.71 a
72	7.86±0.67 a	44.97±4.32 a	8.94±0.20 b	17.37±1.62 b	82.63±1.62 a
84	8.13±0.23 a	44.31±5.29 a	9.99±0.44 ab	18.60±2.28 ab	81.40±2.28 b

[1)] Different coefficients represent multiples of conventional density. K_{leaf}, leaf hydraulic conductance; K_x, leaf hydraulic conductance inside-xylem; K_{ox}, leaf hydraulic conductance outside-xylem; R_x/R_{leaf}, inside-xylem hydraulic resistance/total leaf hydraulic resistance; R_{ox}/R_{leaf}, outside-xylem hydraulic resistance/total leaf hydraulic resistance.
Values are mean±SD (n=8). Significance analysis and test of leaf hydraulic characteristic under different planting densities were carried out, and different letters represented the difference of 0.05 level.

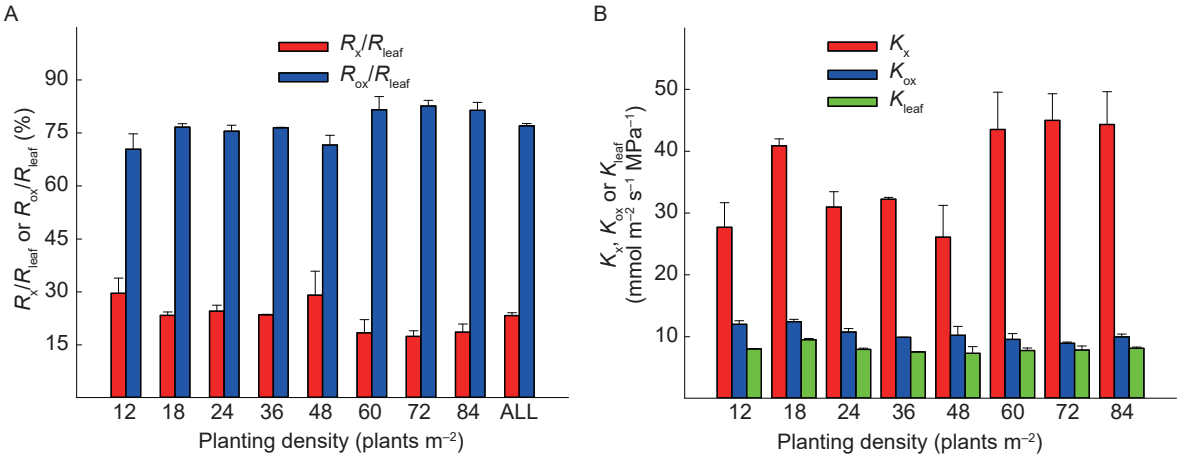


Fig. 1 Percentage of inside-xylem hydraulic resistance (inside-xylem hydraulic resistance (R_x)/total leaf hydraulic resistance (R_{leaf})) (A) and outside-xylem hydraulic resistance (outside-xylem hydraulic resistance (R_{ox})/(R_{leaf}) and leaf hydraulic conductance of inside-xylem (K_x), outside-xylem (K_{ox}) and leaf (K_{leaf}) in different planting densities (B). In A, ALL represents the pooled of the measured parameter mean across all planting density treatments and does not constitute an independent experimental treatment. Values are mean±SD (n=8).

3.3. Influence of leaf hydraulic traits on A_N and WUE

Among all treatments, a decreasing trend in A_N was observed as planting density increased, but there were no significant differences overall. Furthermore, a detailed analysis of leaf intercellular carbon dioxide concentration (C_i) revealed no significant changes in C_i for all planting densities except for the 72 plants m^{-2} (Appendix A). Our study found no correlation between g_s and A_N (Appendix B-a). Furthermore, the investigation into the relationships between K_{leaf}, K_x and K_{ox} with A_N revealed no significant correlation (Appendix B-b–d).

WUE_i was significantly lower at the two lowest planting densities (12 and 18 plants m^{-2}) compared to other planting densities. Similarly, the long-term WUE ($\delta^{13}C$) at these two lowest planting densities was significantly lower than at other planting densities (Appendix A). The analysis of WUE indicated a negative correlation between K_{ox} and WUE_i (Fig. 3-B). Similarly, there was no significant correlation between $\delta^{13}C$ and K_x (Fig. 3-C), but a weak negative correlation was found between $\delta^{13}C$ and K_{ox} (Fig. 3-D; R^2=0.438, P=0.074).

3.4. Impact of leaf hydraulic conductance outside xylem on stomatal structure

To explore the structural basis of the relationship between K_{ox} and g_s, we investigated the relationship between K_x and K_{ox} with SPI. As indicated in Appendix C, planting density significantly affected SPI, with the lowest SPI observed at the lowest planting density (12 plants m^{-2}) and the highest SPI observed at the 24 plants m^{-2}. Overall, SPI exhibited an initial increase followed by a stable trend as planting density increased. Analyzing the relationship between SPI and leaf hydraulic functions revealed no significant correlation between K_x and SPI, as well as between K_x and adaxial SPI and abaxial SPI (Appendix D). In contrast, K_{ox} exhibited a weak negative correlation with SPI (Appendix E-a; R^2=0.349, P=0.123), no correlation with adaxial SPI (Appendix E-b), and a significant negative correlation with abaxial SPI (Appendix E-c).

3.5. Impact of leaf structure on leaf hydraulic conductance outside xylem

To elucidate the impact of leaf structure on hydraulic functionality under different planting densities in the same cotton genotype. We investigated the effects of leaf thickness (LT), palisade tissue thickness (PTT), and spongy tissue thickness (STT) on K_{ox}. The results revealed a negative liner correlation between LT and K_{ox} (Fig. 4-A). There was a significant negative correlation between spongy tissue thickness and K_{ox} (Fig. 4-C).

Furthermore, we analyzed the impact of mesophyll cell area on K_{ox}. The results showed a negative correlation between palisade tissue cell area (PTCA) and K_{ox}, indicating that larger PTCA are associated with lower K_{ox} (Appendix F-a). However, Appendix F-b revealed that spongy tissue cell area (SPCA) had no significant effect on K_{ox}. In addition, we investigated the influence of fraction of leaf mesophyll volume occupied by f_{IAS} on K_{ox}. The results demonstrated a positive correlation between leaf cross-sectional f_{IAS} and K_{ox} (Fig. 5-A). Fraction of leaf palisade tissue volume occupied by intercellular air space (f_{IAS_PT}) showed no significant correlation with K_{ox} (Fig. 5-B), while fraction of leaf spongy tissue volume occupied by intercellular air space (f_{IAS_ST}) exhibited a close relationship with K_{ox} (Fig. 5-C). These findings suggest that as the intercellular space area of mesophyll tissue increases, the water transport efficiency outside the xylem improves when mesophyll tissue porosity increases, with spongy tissue porosity playing a more critical role.

3.6. Correlation analysis and model construction

Principal component analysis was performed for key traits (Fig. 6). The first axis of principal component analysis accounts for 54.3% of the total variation, indicating a strong negative association among f_{IAS}, f_{IAS_ST}, f_{IAS_PT}, g_s, K_{ox}, SPI, $\delta^{13}C$, STT, and WUE_i. The second principal component (PC2) explained 21.2% of the total variation. The PCA results revealed that K_{ox} has a positive influence on g_s but is significantly negatively correlated with WUE. Furthermore, the variation in K_{ox} was positively associated with mesophyll cell porosity but negatively correlated with leaf thickness.

We summarized the influencing factors of water transport

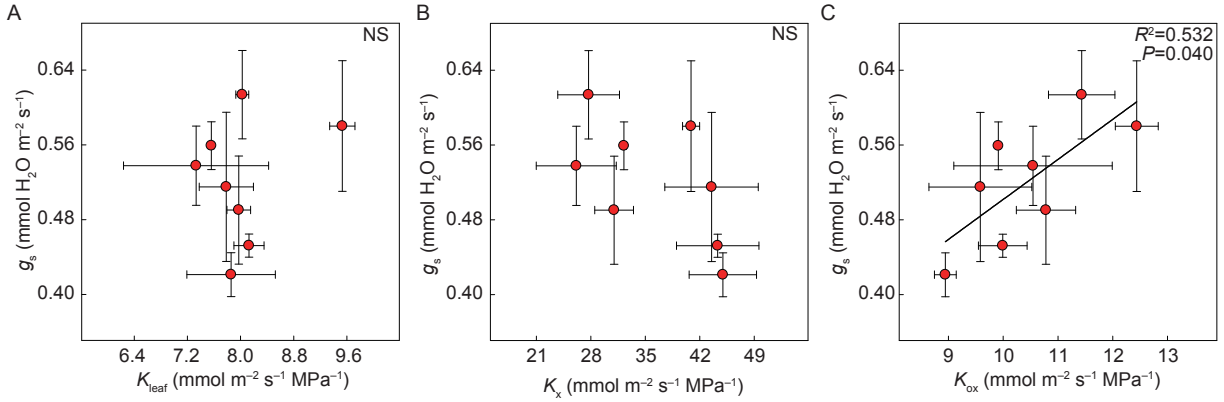


Fig. 2 Correlation between stomatal conductance (g_s) and leaf hydraulic conductance (K_{leaf}) (A) and stomatal conductance (g_s) and leaf hydraulic conductance of inside-xylem (K_x) (B) and stomatal conductance (g_s) and leaf hydraulic conductance of outside-xylem (K_{ox}) (C) in different planting densities. Values are mean±SD (n=8). The fitting lines are shown when P<0.05. NS, not significance.

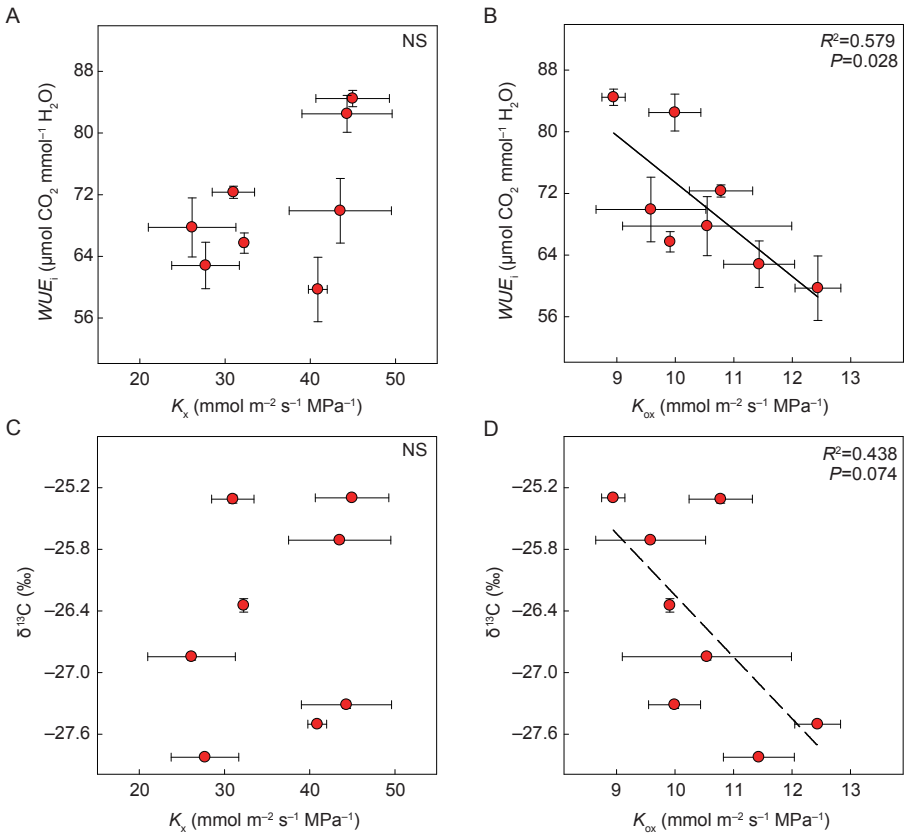


Fig. 3 Correlation between intrinsic water use efficiency (WUE_i) and leaf hydraulic conductance of inside-xylem (K_x) (A) and WUE_i and leaf hydraulic conductance of outside-xylem (K_{ox}) (B), K_x and δ^{13}C (C), and δ^{13}C and K_{ox} (D) in different planting densities. Values are mean±SD (n=8). NS, not significance. The fitting lines are shown when P<0.05.

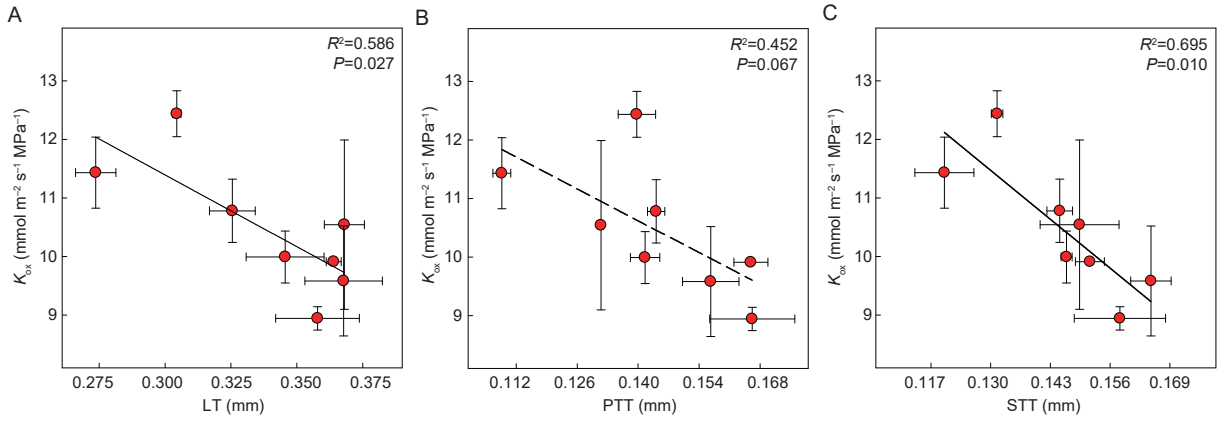


Fig. 4 Effects of leaf thickness (LT) (A), palisade tissue thickness (PTT) (B), spongy tissue thickness (STT) (C) on leaf hydraulic conductance of outside-xylem (K_{ox}) in different planting densities. Values are mean±SD (n=8). The fitting lines are shown when P<0.05.

efficiency and the relationship between water diffusion and WUE in cotton leaves under different planting densities. Fig. 7 illustrates these relationships, with the long triangle in the center depicting the trend of the indicators: an increase from the tip to the edge of the triangle represents an upward trend. We can see that f_{IAS} gradually increases and LT gradually decreases with the increase of planting density (green long triangle). K_{ox} decreased with the increase of planting density, and was positively affected by f_{IAS} and negatively affected by LT. Additionally, a decrease in K_{ox} results in reduced g_s but increased WUE (blue long triangle).

4. Discussion

4.1. Water transport resistance of leaves mainly comes from the water transport path outside the xylem

The pathway of water transport within leaves is complex, and

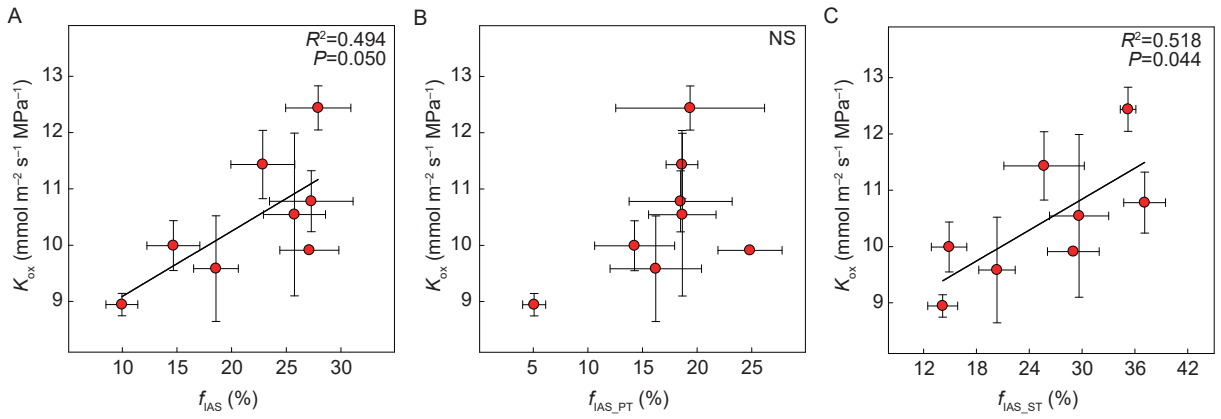


Fig. 5 Effects of fraction of leaf mesophyll volume occupied by intercellular air space (f_{IAS}) (A), fraction of leaf palisade tissue volume occupied by intercellular air space (f_{IAS_PT}) (B), and fraction of leaf spongy tissue volume occupied by intercellular air space (f_{IAS_ST}) on leaf hydraulic conductance of outside-xylem (K_{ox}) (C) in different planting densities. Values are mean±SD (n=8). The fitting lines are shown when P<0.05. NS, not significance.

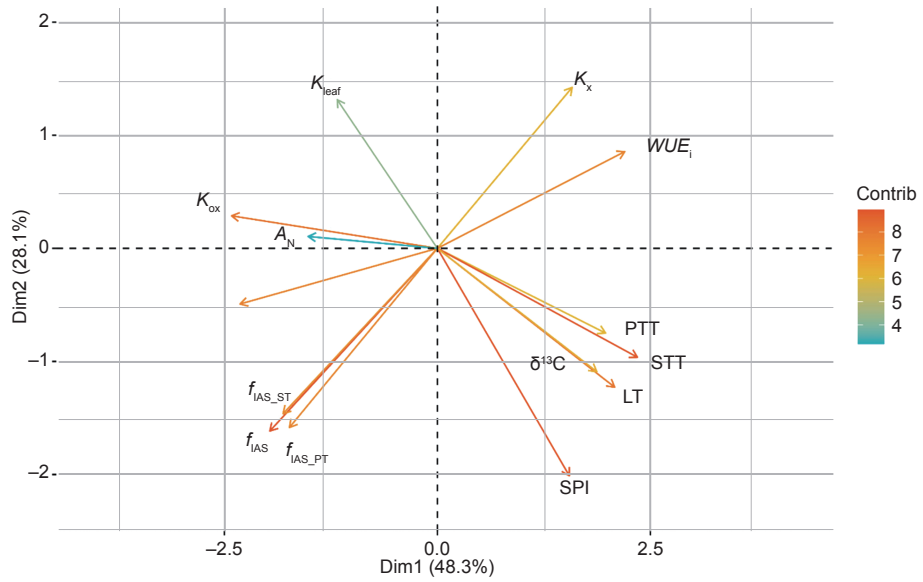


Fig. 6 Principal component analysis (PCA) of leaf functional and structural traits. K_{leaf}, leaf hydraulic conductance; K_x, leaf hydraulic conductance inside-xylem; K_{ox}, leaf hydraulic conductance outside-xylem; A_N, leaf photosynthetic rate; g_s, stomatal conductance; f_{IAS}, leaf mesophyll volume occupied by intercellular air space; f_{IAS_PT}, fraction of leaf palisade tissue volume occupied by intercellular air space; f_{IAS_ST}, fraction of leaf spongy tissue volume occupied by intercellular air space; SPI, stomatal pore area index; WUE_i, inherent water use efficiency; δ^{13}C, stable isotope ^{13}C ratio; LT, leaf thickness; PTT, palisade tissue thickness; STT, spongy tissue thickness.

extensive variation in K_{leaf} reported across different species and environmental conditions (Sack and Holbrook 2006). This variation has been present in cultivated crops (Xiong *et al.* 2017). However, our study results indicated a high degree of conservatism in K_{leaf} for the same cotton genotype under different planting densities (Table 1). Surprisingly, despite the conservatism in K_{leaf}, planting density led to adaptive adjustments in K_x and K_{ox} (Table 1). Furthermore, partitioning total hydraulic resistance (R_{leaf}=1/K_{leaf}) into the inside-xylem and outside-xylem components is a crucial step in understanding leaf hydraulic design. Relative hydraulic resistance provides a clearer description of the contributions of K_x and K_{ox} to the leaf's overall hydraulic properties. In our results, hydraulic resistance within the xylem ranged from 17.37 to 29.58%, with an average of 23.08%, while hydraulic resistance outside the xylem ranged from 70.41 to 82.63%, with an average of 77.03%. This suggests that planting density influences the relative contributions of R_x and R_{ox} to hydraulic resistance in leaves. Moreover, cotton leaf hydraulic resistance was primarily attributed to the outside-xylem water transport pathway at different cultivation densities (Table 1; Fig. 1). This finding is consistent with previous research on the allocation of hydraulic resistance within leaves, where hydraulic resistance inside-xylem and outside-xylem had been of similar magnitude and significantly different among species (Sack *et al.* 2004; Nardini *et al.* 2005;

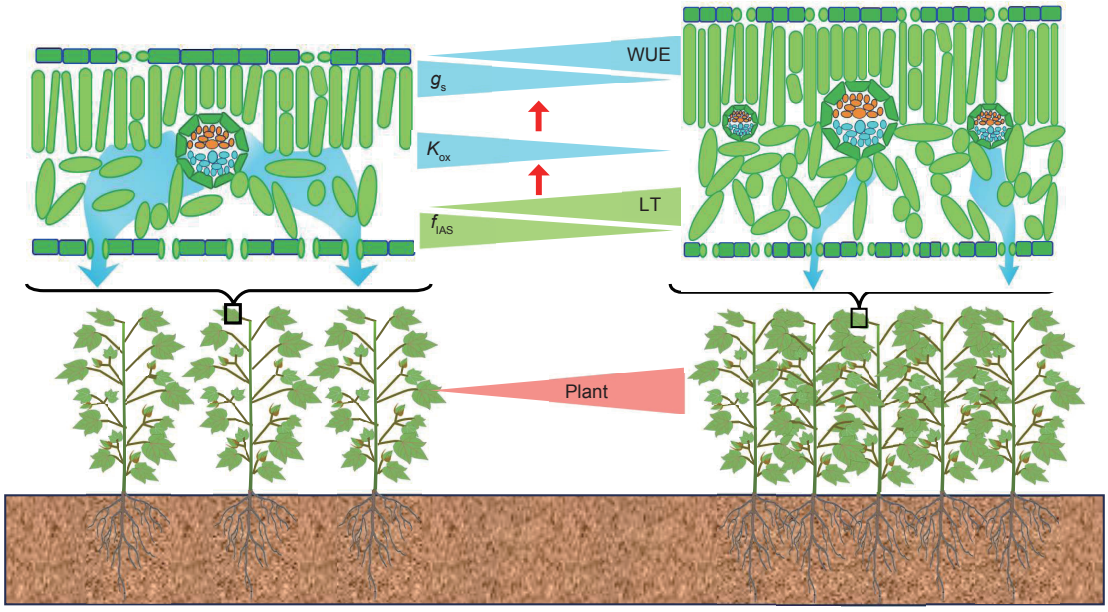


Fig. 7 Structural limiting basis of water transport in cotton leaves and the regulating relationship between water diffusion and water use efficiency (WUE). The point of the long triangle points in the direction of the decreasing value. The direction pointed by the small red arrow indicates that the arrow tail character has an effect on the arrow character. f_{IAS}, leaf mesophyll volume occupied by intercellular air space; LT, leaf thickness; K_{ox}, leaf hydraulic conductance outside-xylem; g_s, stomatal conductance.

Sack *et al.* 2005). For instance, Sack *et al.* (2005) found that the percentage of hydraulic resistance in the extraxylem ranged from 11 to 74% in 10 tropical rainforest tree species. In our results, there was no significant difference in main vein density among the planting density treatments, while small vein density showed a significant difference (Appendix H). Additionally, the major veins in reticulate venation plants primarily provide mechanical support with lower flow resistance (Sack *et al.* 2004). Therefore, we considered only veins of the 3rd order and above, excluding the major veins in our calculations for K_x.

4.2. Hydraulic conductance outside xylem is the main reason limiting the g_s of leaves

The coupling of K_{leaf} and A_N has been widely observed, and the coordination between K_{leaf} and A_N is influenced by g_s (Brodribb *et al.* 2007; Brodribb and Jordan 2008). In our results, the primary factor affecting g_s was K_{ox} rather than K_{leaf} or K_x (Fig. 2), which is similar to the findings of Lu *et al.* (2019) in different potassium supply conditions for monocots and dicots. Clearly, outside-xylem water transport resistance in the leaf veins represents the major factor limiting g_s under different planting densities of the same cotton genotype. This can be understood for several reasons. Firstly, our results showed that outside-xylem resistance is the predominant contributor to overall leaf hydraulic resistance. Secondly, leaf veins are situated within the mesophyll and are separated from the guard cells by a certain distance. The transport of water from leaf veins to stomata involves symplastic transport pathways between bundle sheath cells. In contrast, the extravascular water transport pathways are closer to the guard cells. Therefore, the influence of K_{ox} on g_s at hydraulic distance should be more direct. Additionally, K_x typically exhibits daily fluctuations (Meinzer *et al.* 2008) and seasonal changes (Prior and Eamus 2000; Brodribb *et al.* 2002). Moreover, K_x is primarily influenced by leaf vein structure, including VLA, the number of conduits, and individual conduit diameter (Sack and Frole 2006; Sack and Holbrook 2006). Furthermore, recent research has shown that leaf vein conduit structure can undergo elastic deformation in response to leaf water status, which is directly related to leaf hydraulic efficiency (Verslues *et al.* 2023). Therefore, it can be inferred that the leaf vein system incorporates redundancy under varying planting densities. Thus, a decrease in K_x does not necessarily reduce g_s which can also lead to decoupling between K_x and g_s.

4.3. There is a coupling relationship between leaf hydraulic conductance outside xylem and WUE

Our results indicate that neither K_x nor K_{ox} impacted on A_N (Appendix B-c and d). And, A_N showed no significant correlation with g_s (Appendix B-a), and the analysis of C_i revealed no significant differences between treatments (Appendix A). This suggest that although the ability of mesophyll cells to transport carbon dioxide differs (Tosens *et al.* 2016), thereby maintaining stable leaf photosynthetic rates at high densities. Secondly, we observed that high planting density was associated with a higher SPI (Appendix C), enhancing the regulatory capacity of stomata structurally (Liu *et al.* 2018; Ramírez-Valiente *et al.* 2018). Furthermore, guard cells not only contain chloroplasts (Talbott and Zeiger 1998) but also have photosynthetic capacity, enabling direct control of stomatal movement (Ueno 2001; Zeiger *et al.* 2002; Outlaw 2003). Therefore, maintaining a high guard cell surface area at high densities enhances stomatal regulation capacity and facilitates carbon assimilation due to the location of stomata at the forefront of the leaf, resulting in a decoupling of A_N rate

from g_s. Further, K_{ox} was found to regulate WUE_i (Fig. 3-B), and the relationship between $\delta^{13}C$ and K_{ox} supports this result (Fig. 3-D). The increase in K_{ox} leads to an increase in water loss through stomata (g_s) (Fig. 2-C), thereby reducing WUE, which is easily understandable. However, what we should pay more attention to is that as K_{ox} increases, SPI decreases (Appendix E). The ability of leaves to adjust stomata is weak, and the WUE is reduced under the treatment of lower SPI (Liu *et al.* 2018). More importantly, unlike mesophyll cells, guard cells' photosynthesis comes at the cost of less water loss due to their unique position on the leaf. Therefore, leaves with higher SPI are expected to have higher WUE. However, the extent to which the increase in SPI benefits cotton A_N and WUE requires further in-depth research.

4.4. Thickness and porosity of spongy tissue are the anatomical basis that determine the leaf hydraulic conductance outside the xylem

Our research findings indicate that as leaf thickness increases, K_{ox} decreases (Fig. 4-A), particularly with respect to the thickness of the spongy tissue (Fig. 4-C). However, previous studies on the impact of leaf thickness on K_{ox} have yielded inconsistent results, with thicker leaves frequently believed to enhance both K_{leaf} and K_{ox} (Zhang and Cao 2009; Gao *et al.* 2023). This observation may be attributed to the additional parallel pathways for horizontal transport provided by thicker leaves, which reduce resistance. However, the study by suggests that K_{ox} is unrelated to leaf thickness, and modeling simulations indicate that variations in leaf thickness among different species have minimal effects on leaf water transport efficiency. Our results show that the increase of leaf thickness with the increase of planting density lengthens the water transport path within the same cotton variety, resulting in an increase in water transport resistance. Although thicker leaves can offer additional water transport pathways (de Boer *et al.* 2016). But thickened leaves allow water to travel farther, increasing water flow resistance of mesophyll tissue. Furthermore, an increase in leaf thickness reduces temperature gradients within the leaves, significantly affecting K_{ox}. For instance, K_{ox} increases by 16 to 65% on average as the internal temperature gradient within the leaves rises from 0°C to 0.2°C (Buckley *et al.* 2015).

Furthermore, in our results, the thickness of the spongy tissue has a greater impact on K_{ox} (Fig. 4). This effect may be attributed to the fact that stomata are primarily distributed on the abaxial surface of cotton leaves (Appendix C). Consequently, the increased water loss from the abaxial surface enhances the influence of the spongy tissue structure on K_{ox} (Buckley *et al.* 2015). Clearly, the effect of leaf thickness on water transport efficiency varies under different conditions. However, it is known that there are underlying mechanisms linking leaf anatomy and leaf thickness, resulting in changes in mesophyll cell properties and intercellular connectivity. Further analysis of mesophyll cell size reveals that although changes in spongy tissue thickness significantly affect K_{ox} (Fig. 4-C), the cell area of spongy tissue is not the primary factor influencing K_{ox} (Appendix F-b). Conversely, with an increase in the cell area of palisade tissue, K_{ox} significantly decreases (Appendix F-a). Our data demonstrate a correlation between the increase in palisade tissue cell size and the increase in palisade tissue thickness (Appendix H). Therefore, the reduction in K_{ox} due to the increase in cell area of palisade tissue is likely attributed to the association between leaf anatomy components. Specifically, the increase in palisade tissue thickness leads to an increase in palisade tissue cell area, prolonging the water transport pathway and increasing water transport resistance (John *et al.* 2013). Additionally, we observed that the cell size of spongy tissue remains relatively constant under different planting densities of the same cotton species, indicating the conservativeness of spongy tissue cell size (Table 2). This result differs from the findings of Buckley *et al.* (2015) and John *et al.* (2013), suggesting that the conservativeness ofspongy cell size may represent a new adaptation strategy in cotton to respond to environmental changes. Changes in mesophyll cell size can lead to variations in the porosity of palisade and spongy tissues. Our results revealed a positive correlation between leaf cross-sectional f_{IAS} and K_{ox}, primarily mediated by the f_{IAS_ST}, with limited association with f_{IAS_PT} (Fig. 5). After water flows out of the xylem, it enters stomata through intercellular spaces, symplast, membranes, and gas-phase pathways. The apoplastic pathway is believed to dominate external water transport. Therefore, the increase in the porosity of mesophyll tissue, particularly the spongy tissue, enhances the surface area for cell evaporation while reducing the area available for liquid-phase flow, thereby increasing K_{ox}. The resistance to apoplastic water transport is considerably lower than that of symplastic water transport.

5. Conclusion

Our research results indicate that the overall leaf hydraulic efficiency remains constant in the same genotype under different planting densities. However, there were significant changes in both inside xylem and outside xylem water transport efficiencies, with outside xylem water transport efficiency being the primary limiting factor of overall leaf hydraulic efficiency and a crucial factor in regulating water use efficiency through stomatal conductance. The outside xylem water transport efficiency was influenced by leaf thickness, particularly the thickness of the spongy tissue. Nonetheless, the increase in porosity of the spongy tissue enhances outside xylem water transport efficiency. This study reveals the structural constraints underlying K_{ox} and its key role in regulating stomatal conductance and water use efficiency. It holds significant practical implications for future efforts to manipulate crop water use efficiency through cultivation and breeding approaches.

Acknowledgements

This research was financially supported by the Tianshan Talent Development Program, China for Yali Zhang, the Natural Science Foundation of Xinjiang Production and Construction Corps, China (2024DA002), the Earmarked Fund for XJARS-Cotton, China (XJARS-03).

Table 2 Effect of planting density (PD) on leaf anatomy structure characters[1)]

PD (plants m^{-2})	LT (mm)	PTT (mm)	STT (mm)	PTCA (×10^2 μm^2)	STCA (×10^2 μm^2)	f_{IAS} (%)	f_{IAS_PT} (%)	f_{IAS_ST} (%)
12	0.274±0.008 d	0.109±0.002 d	0.120±0.006 c	10.75±1.98 e	4.41±0.44 a	22.85±2.92 ab	18.62±1.45 a	25.68±4.56 b
18	0.304±0.002 c	0.140±0.004 abc	0.131±0.001 c	12.53±0.78 de	4.78±0.49 a	27.92±2.98 a	19.36±6.81 a	35.22±0.89 a
24	0.326±0.009 bc	0.144±0.002 b	0.145±0.003 b	15.24±1.29 cd	4.36±0.13 a	27.29±3.83 a	18.49±4.71 a	37.11±2.37 a
36	0.364±0.003 a	0.166±0.004 a	0.152±0.003 ab	15.84±0.53 cd	4.37±0.08 a	27.11±2.70 a	24.84±2.94 a	29.01±2.94 b
48	0.368±0.008 a	0.131±0.001 bc	0.149±0.009 b	13.44±0.44 de	4.66±0.25 a	25.75±2.84 a	18.65±3.08 a	29.66±3.36 b
60	0.368±0.015 a	0.157±0.006 a	0.165±0.004 a	18.18±1.30 bc	4.58±0.45 a	18.57±2.05 bc	16.21±4.18 a	20.33±2.06 c
72	0.358±0.016 a	0.166±0.010 a	0.158±0.010 ab	19.38±0.89 b	4.55±0.33 a	9.96±1.45 d	5.08±1.05 b	14.16±1.70 d
84	0.346±0.015 ab	0.142±0.003 bc	0.147±0.001 b	23.54±2.03 a	4.75±0.16 a	14.66±2.42 cd	14.28±3.67 ab	14.89±2.01 d

[1)] Different coefficients represent multiples of conventional density. LT, leaf thickness; PTT, palisade tissue thickness; STT, spongy tissue thickness; PTCA, palisade tissue cell area; STCA, spongy tissue cell area; f_{IAS}, fraction of leaf mesophyll volume occupied by intercellular air space; f_{IAS_PT}, fraction of leaf palisade tissue volume occupied by intercellular air space; f_{IAS_ST}, fraction of leaf spongy tissue volume occupied by intercellular air space.
Values are mean±SD (n=8). The significance analysis and test of leaf vascular bundle structure parameters under different planting densities were carried out, and different letters represented the difference of 0.05 level.

Declaration of competing interest

The authors declare that they have no conflict of interest.

Declaration of generative AI and AI-assisted technologies in the writing process

During the preparation of this manuscript, the authors used ChatGPT 4.0 to assist in improving the clarity and readability of the language. All content generated was carefully reviewed and revised by the authors as necessary, and the authors take full responsibility for the final content of the article.

Appendices associated with this paper are available at https://doi.org/10.1016/j.jia.2024.11.012

References

Aasamaa K, Sober A, Rahi M. 2001. Leaf anatomical characteristics associated with shoot hydraulic conductance, stomatal conductance and stomatal sensitivity to changes of leaf water status in temperate deciduous trees. *Australian Journal of Plant Physiology*, **28**, 765–774.

Blonder B, Violle C, Bentley L P, Enquist B J. 2011. Venation networks and the origin of the leaf economics spectrum. *Ecology Letters*, **14**, 91–100.

de Boer H J, Drake P L, Wendt E, Price C A, Schulze E D, Turner N C, Nicolle D, Veneklaas E J. 2016. Apparent overinvestment in leaf venation relaxes leaf morphological constraints on photosynthesis in arid habitats. *Plant Physiology*, **172**, 2286–2299.

Boyer J S. 1974. Water transport in plants: Mechanism of apparent changes in resistance during absorption. *Planta*, **117**, 187–207.

Brodribb T J, Feild T S, Jordan G J. 2007. Leaf maximum photosynthetic rate and venation are linked by hydraulics. *Plant Physiology*, **144**, 1890–1898.

Brodribb T J, Holbrook N M, Gutierrez M V. 2002. Hydraulic and photosynthetic co-ordination in seasonally dry tropical forest trees. *Plant Cell and Environment*, **25**, 1435–1444.

Brodribb T J, Jordan G J. 2008. Internal coordination between hydraulics and stomatal control in leaves. *Plant Cell and Environment*, **31**, 1557–1564.

Buckley T N, John G P, Scoffoni C, Sack L. 2015. How does leaf anatomy influence water transport outside the xylem? *Plant Physiology*, **168**, 1616–1635.

Cochard H, Nardini A, Coll L. 2004. Hydraulic architecture of leaf blades: Where is the main resistance? *Plant*, **27**, 1257–1267.

Corrêa F F, Madail R H, Barbosa S, Pereira M P, Castro E M, Soriano C T G, Pereira F J. 2015. Anatomy and physiology of Cattail as related to different population densities. *Planta Daninha*, **33**, 1–12.

Corso D, Delzon S, Lamarque L J, Cochard H, Torres-Ruiz J M, King A, Brodribb T. 2020. Neither xylem collapse, cavitation, or changing leaf conductance drive stomatal closure in wheat. *Plant*, **43**, 854–865.

Farquhar G, Richards R. 1984. Isotopic composition of plant carbon correlates with water-use efficiency of wheat genotypes. *Functional Plant Biology*, **11**, 539–552.

Gao J, Chen J Y, Lei Y, Wang Q, Zou J Q, Ning Z L, Tan X M, Yang F, Yang W Y. 2023. Functional consequences of light intensity on soybean leaf hydraulic conductance: Coordinated variations in leaf venation architecture and mesophyll structure. *Environmental and Experimental Botany*, **210**, 105301.

Gonzalez J A, Mercado M I, Martinez-Calsina L, Erazz L E, Buedo S E, Gonzalez D A, Ponessa G I. 2022. Plant density effects on quinoa yield, leaf anatomy, ultrastructure and gas exchange. *Journal of Agricultural Science*, **160**, 349–359.

Huang G J, Zhang Q Q, Wei X H, Peng S, Li Y. 2017. Nitrogen can alleviate the inhibition of photosynthesis caused by high temperature stress under both steady-state and flecked irradiance. *Frontiers in Plant Science*, **8**, 945.

John G P, Scoffoni C, Sack L. 2013. Allometry of cells and tissues within leaves. *American Journal of Botany*, **100**, 1936–1948.

Maria J H, Fernando M, Federico R, Gustavo L, Pilar P. 2016. The effect of vapour pressure deficit on stomatal conductance, sap pH and leaf-specific hydraulic conductance in *Eucalyptus globulus* clones grown under two watering regimes. *Annals of Botany*, **117**, 1063–1071.

Liu C, He N, Zhang J, Li Y, Wang Q, Sack L, Yu G. 2018. Variation of stomatal traits from cold temperate to tropical forests and association with water use efficiency. *Functional Ecology*, **32**, 20–28.

Liu X R, Liu H, Gleason S M, Goldstein G, Zhu S D, He P C, Hou H, Li R H, Ye Q. 2019. Water transport from stem to stomata: The coordination of hydraulic and gas exchange traits across 33 subtropical woody species. *Tree Physiology*, **39**, 1665–1674.

Locke A M, Ort D R. 2014. Leaf hydraulic conductance declines in coordination with photosynthesis, transpiration and leaf water status as soybean leaves age regardless of soil moisture. *Journal of Experimental Botany*, **65**, 6617–6627.

Lu Z F, Xie K L, Pan Y H, Ren T, Lu J W, Wang M, She Q R, Guo S W. 2019. Potassium mediates coordination of leaf photosynthesis and hydraulic conductance by modifications of leaf anatomy. *Plant Cell and Environment*, **42**, 2231–2244.

Meidner H. 1976. Water vapour loss from a physical model of a substomatal cavity. *Journal of Experimental Botany*, **27**, 691–694.

Meinzer F C, Woodruff D R, Domec J C, Goldstein G, Campanello P I, Gatti M G, Villalobos-Vega R. 2008. Coordination of leaf and stem water transport properties in tropical forest trees. *Oecologia*, **156**, 31–41.

Nardini A, Gortan E, Salleo S. 2005. Hydraulic efficiency of the leaf venation system in sun- and shade-adapted species. *Functional Plant Biology*, **32**, 953–961.

North G B, Lynch F H, Maharaj F D R, Phillips C A, Woodside W T. 2013. Leaf hydraulic conductance for a tank bromeliad: Axial and radial pathways for moving and conserving water. *Frontiers in Plant Science*, **4**, 78.

Ocheltree T W, Nippert J B, Prasad P V V. 2016. A safety vs efficiency trade-off identified in the hydraulic pathway of grass leaves is decoupled from photosynthesis, stomatal conductance and precipitation. *The New Phytologist*, **210**, 97–107.

Outlaw W H. 2003. Integration of cellular and physiological functions of guard cells. *Critical Reviews in Plant Sciences*, **22**, 503–529.

Pittermann J, Limm E, Rico C, Christman M A. 2011. Structure–function constraints of tracheid-based xylem: A comparison of conifers and ferns. *New Phytologist*, **192**, 449–461.

Prior L D, Eamus D. 2000. Seasonal changes in hydraulic conductance, xylem embolism and leaf area in *Eucalyptus tetrodonta* and *Eucalyptus miniata* saplings in a north Australian savanna. *Plant Cell and Environment*, **23**, 955–965.

Ramírez-Valiente J A, Deacon N J, Etterson J, Center A, Sparks J P, Sparks K L, Longwell T, Pilz G, Cavender-Bares J. 2018. Natural selection and neutral evolutionary processes contribute to genetic divergence in leaf traits across a precipitation gradient in the tropical oak *Quercus oleoides*. *Molecular Ecology*, **27**, 2176–2192.

Ruiz R A, Bertero H D. 2008. Light interception and radiation use efficiency in temperate quinoa (*Chenopodium quinoa* Willd.) cultivars. *European Journal of Agronomy*, **29**, 144–152.

Sack L, Cowan P D, Jaikumar N, Holbrook M. 2003. The 'Hydrology' of leaves: Co-ordination of structure and function in temperate woody species. *Plant*, *Cell & Environment*, **26**, 1343–1356.

Sack L, Dietrich E M, Streeter C M, Sanchez-Gomez D, Holbrook N M. 2008. Leaf palmate venation and vascular redundancy confer tolerance of hydraulic disruption. *Proceedings of the National Academy of Sciences of the United States of America*, **105**, 1567–1572.

Sack L, Frole K. 2006. Leaf structural diversity is related to hydraulic capacity in tropical rain forest trees. *Ecology*, **87**, 483–491.

Sack L, Holbrook N M. 2006. Leaf hydraulics. *Annual Review of Plant Biology*, **57**, 361–381.

Sack L, Melcher P J, Zwieniecki M A, Holbrook N M. 2002. The hydraulic conductance of the angiosperm leaf lamina: A comparison of three measurement methods. *Journal of Experimental Botany*, **53**, 2177–2184.

Sack L, Scoffoni C. 2012. Measurement of leaf hydraulic conductance and stomatal conductance and their responses to irradiance and dehydration using the evaporative flux method (EFM). *Jove-Journal of Visualized Experiments*, **70**, 4179.

Sack L, Streeter C M, Holbrook N M. 2004. Hydraulic analysis of water flow through leaves of sugar maple and red oak. *Plant Physiology*, **134**, 1824–1833.

Sack L, Tyree M T, Holbrook N M. 2005. Leaf hydraulic architecture correlates with regeneration irradiance in tropical rainforest trees. *New Phytologist*, **167**, 403–413.

Salleo S, Raimondo F, Trifilo P, Nardini A. 2003. Axial-to-radial water permeability of leaf major veins: A possible determinant of the impact of vein embolism on leaf hydraulics? *Plant Cell and Environment*, **26**, 1749–1758.

Scoffoni C. 2015. Modelling the outside-xylem hydraulic conductance: Towards a new understanding of leaf water relations. *Plant*, *Cell & Environment*, **38**, 4–6.

Scoffoni C, Chatelet D S, Pasquet-kok J, Rawls M, Donoghue M J, Edwards E J, Sack L. 2016. Hydraulic basis for the evolution of photosynthetic productivity. *Nature Plants*, **2**, 16072.

Scoffoni C, Sack L. 2015. Are leaves 'freewheelin'? Testing for a Wheeler-type effect in leaf xylem hydraulic decline. *Plant Cell and Environment*, **38**, 534–543.

Sterck F J, Zweifel R, Sass-Klaassen U, Chowdhury Q. 2008. Persisting soil drought reduces leaf specific conductivity in Scots pine (*Pinus sylvestris*) and pubescent oak (*Quercus pubescens*). *Tree Physiology*, **28**, 529–536.

Sun S J, Chen Z J, Jiang H, Zhang X D, Zhang L L, Chi D C. 2019. Plastic mulch and plant density influencing soil water content and yield of rainfed maize in North-Eastern China. *Irrigation and Drainage*, **68**, 354–364.

Talbott L D, Zeiger E. 1998. The role of sucrose in guard cell osmoregulation. *Journal of Experimental Botany*, **49**, 329–337.

Theroux-Rancourt G, Ethier G, Pepin S. 2013. Threshold response of mesophyll CO_2 conductance to leaf hydraulics in highly transpiring hybrid poplar clones exposed to soil drying. *Journal of Experimental Botany*, **65**, 741–754.

Toillon J, Fichot R, Dallé E, Berthelot A, Brignolas F, Marron N. 2013. Planting density affects growth and water-use efficiency depending on site in *Populus deltoides*×*P. nigra*. *Forest Ecology and Management*, **304**, 345–354.

Tosens T, Nishida K, Gago J, Coopman R E, Cabrera H M, Carriquí M, Laanisto L, Morales L, Nadal M, Rojas R, Talts E, Tomas M, Hanba Y, Niinemets Ü, Flexas J. 2016. The photosynthetic capacity in 35 ferns and fern allies: Mesophyll CO_2 diffusion as a key trait. *New Phytologist*, **209**, 1576–1590.

Trifilo P, Nardini A, Lo Gullo M A, Salleo S. 2003. Vein cavitation and stomatal behaviour of sunflower (*Helianthus annuus*) leaves under water limitation. *Physiologia Plantarum*, **119**, 409–417.

Tyree M T, Yianoulis P. 1980. The site of water evaporation from sub-stomatal cavities, liquid path resistances and hydroactive stomatal closure. *Annals of Botany*, **46**, 175–193.

Ueno O. 2001. Ultrastructural localization of photosynthetic and photorespiratory enzymes in epidermal, mesophyll, bundle sheath, and vascular bundle cells of the C_4 dicot *Amaranthus viridis*. *Journal of Experimental Botany*, **52**, 1003–1013.

Ueno O, Kawano Y, Wakayama M, Takeda T. 2006. Leaf vascular systems in C_3 and C_4 grasses: A two-dimensional analysis. *Annals of Botany*, **97**, 611–621.

Verslues P E, Bailey-Serres J, Brodersen C, Buckley T N, Conti L, Christmann A, Dinneny J R, Grill E, Hayes S, Heckman R W, Hsu P K, Juenger T E, Mas P, Munnik T, Nelissen H, Sack L, Schroeder J, Testerink C, Tyerman S D, Umezawa T, *et al.* 2023. Burning questions for a warming and changing world: 15 unknowns in plant abiotic stress. *Plant Cell*, **35**, 67–108.

Xiong D, Douthe C, Flexas J. 2018. Differential coordination of stomatal conductance, mesophyll conductance, and leaf hydraulic conductance in response to changing light across species. *Plant Cell and Environment*, **41**, 436–450.

Xiong D, Flexas J, Yu T, Peng S, Huang J. 2017. Leaf anatomy mediates coordination of leaf hydraulic conductance and mesophyll conductance to CO_2 in *Oryza*. *New Phytologist*, **213**, 572–583.

Xiong D L, Yu T T, Zhang T, Li Y, Peng S B, Huang J L. 2015. Leaf hydraulic conductance is coordinated with leaf morpho-anatomical traits and nitrogen status in the genus *Oryza*. *Journal of Experimental Botany*, **66**, 741–748.

Yang H W, Chai Q, Yin W, Hu F L, Qin A Z, Fan Z L, Yu A Z, Zhao C, Fan H. 2022. Yield photosynthesis and leaf anatomy of maize in inter- and mono-cropping systems at varying plant densities. *Crop Journal*, **10**, 893–903.

Yao H S, Zhang Y L, Yi X P, Zhang X J, Zhang W F. 2016. Cotton responds to different plant population densities by adjusting specific leaf area to optimize canopy photosynthetic use efficiency of light and nitrogen. *Field Crops Research*, **188**, 10–16.

Zeiger E, Talbott L D, Frechilla S, Srivastava A, Zhu J X. 2002. The guard cell chloroplast: A perspective for the twenty-first century. *New Phytologist*, **153**, 415–424.

Zhang D, Luo Z, Li W, Dong H. 2016. Effects of deficit irrigation and plant density on the growth, yield and fiber quality of irrigated cotton. *Field Crops Research*, **197**, 1–9.

Zhang J L, Cao K F. 2009. Stem hydraulics mediates leaf water status, carbon gain, nutrient use efficiencies and plant growth rates across dipterocarp species. *Functional Ecology*, **23**, 658–667.

Executive Editor-in-Chief Shaokun Li
Managing Editor Ning Wang